Tuned amperometric detection of NADH by allosteric modulation of the p-hydroxyphenylacetate reductase C1-hpah immobilized within a redox polymer

Somjai Teanphonkrang, Salome Janke, Pimchai Chaiyen, Jeerus Sucharitakul, Wipa Suginta, Panida Khunkaewla, Wolfgang Schuhmann, Adrian Ruff, and Albert Schulte

Anal. Chem., **Just Accepted Manuscript** • DOI: 10.1021/acs.analchem.7b05467 • Publication Date (Web): 10 Apr 2018

Tuned amperometric detection of NADH by allosteric modulation of the *p*-hydroxyphenylacetate reductase C1-hpah immobilized within a redox polymer

Somjai Teanphonkrang,[1] Salome Janke,[2] Pimchai Chaiyen,[3] Jeerus Sucharitakul,[4] Wipa Suginta,[1,5] Panida Khunkaewla,[1] Wolfgang Schuhmann,[2] Adrian Ruff,[2,*] Albert Schulte[3,*]

[1]School of Chemistry, Institute of Science, Biochemistry - Electrochemistry Research Unit (BECRU), Suranaree University of Technology, 30000 Nakhon Ratchasima, Thailand. [2]Analytical Chemistry - Center for Electrochemical Sciences (CES), Ruhr-University Bochum, 44780 Bochum, Germany. [3]School of Biomolecular Science and Engineering (BSE), Vidyasirimedhi Institute of Science and Technology (VISTEC), 21210 Rayong, Thailand. [4]Department of Biochemistry, Faculty of Dentistry, Chulalongkorn University, 10330 Bangkok, Thailand. [5]Center of Excellence (CoE) in Advanced Functional Materials, Institute of Science, Suranaree University of Technology, Nakhon Ratchasima 30000, Thailand.

Corresponding Author

*Phone: +49-234-3225586 (A.R.); +66-8737-58518 (A.S.).

*Email: adrian.ruff@ruhr-uni-bochum.de (A.R.); albert.s@vistec.ac.th (A.S.).

ABSTRACT: We report the fabrication of an amperometric NADH biosensor system that employs an allosterically modulated bacterial reductase in an adapted Osmium(III)-complex modified redox polymer film for analyte quantification. Chains of complexed Os(III)-centers along matrix polymer strings make electrical connection between the immobilized redox protein and a graphite electrode disc, transducing enzymatic oxidation of NADH into a biosensor current. Sustainable anodic signaling required (1) a redox polymer with a formal potential that matched the redox switch of the embedded reductase and avoided interfering redox interactions and (2) formation of a crosslinked enzyme/polymer film for stable biocatalyst entrapment. The activity of the chosen reductase is enhanced upon binding of an effector, i.e. *p*-hydroxyphenylacetic acid (*p*-HPA), allowing the acceleration of the substrate conversion rate on the sensor surface by in-situ addition or pre-incubation with *p*-HPA. Acceleration of NADH oxidation amplified the response of the biosensor, with a 1.5-fold increase in the sensitivity of analyte detection, compared to operation without the allosteric modulator. Repetitive quantitative testing of solutions of known NADH concentration verified the performance in terms of reliability and analyte recovery. We herewith established the use of allosteric enzyme activation and redox polymer-based enzyme electrode wiring for substrate biosensing, a concept that may be applicable to other allosteric enzymes.

INTRODUCTION

In recent years, allosteric enzymes have received much attention in various research fields such as drug design and the development of protein switches or biosensors [1–5]. The activity of such enzymes is modulated by the binding of an allosteric effector such as specific ligands, ions or proteins. [1–3,6,7] Applications of allosteric proteins in biosensing include the detection of drugs [8], biomarkers [9], cells [10], antibodies [11], DNA [12], carbohydrates [4], pesticides [13], hormone receptor ligands [14], and the specification of metal ions [15]. Moreover, allosteric signal modulation in sensors and catalytic devices was achieved not only with natural effector/protein couples but also with synthetic supramolecular/organometallic systems that were subject to molecular activity stimulation. [3,16,17].

Allosteric enzyme biosensing is usually applied to molecular species that modulate the rate of substrate conversion, which in turn is monitored by suitable physicochemical transducers.[2,3] In this configuration, the onset and magnitude of the change in the signal amplitude indicate the presence or absence of analyte and its concentration, respectively. Employing this principle, Wollenberger and Scheller, for instance, designed an electrochemical biosensor for the analysis of glycogen phosphorylase b (GPB), a heart muscle cell constituent and primary ischemia biomarker that is regulated both through allosteric control by adenosine monophosphate (AMP) and through

phosphorylation.[18] The authors used a three-enzyme cascade that involved functional cooperation between GPB and an alkaline phosphatase (AP)/glucose oxidase (GOx) supplementation to the biosensor immobilization matrix, translating GPB action on glycogen into a quantifiable anodic hydrogen peroxide sensor current. Although GPB was coupled to the sensor surface indirectly through secondary (AP) and tertiary (GOx) enzymes, this early study proved that the concept of allosteric enzyme electroanalysis was feasible for both activator and enzyme substrate detection.

In the case of biosensors employing allosteric redox enzymes, direct electrical connection of the protein to the signal-generating transducer interface is preferable to cascade detection schemes with multiple enzymes. Activatory and inhibitory allosteric modulation of redox enzymes have been reported for a number of systems, for example brain cytochrome P450 46A1 activation by neuroactive compounds[19], 3-hydroxy-3-methyl-glutaryl-coenzyme A reductase inhibition by corrole, an natural tetrapyrolle-based antioxidant[20] and control of Cu-containing bacterial nitrate reductase by exogenous organo-chemical ligands[21]. However, utilization of the allosteric behavior of redox enzymes for quantitative amperometric or voltammetric electroanalysis is, to the best of our knowledge, limited to one proof-of-principle study that used sophisticated protein engineering to convert a PQQ-glucose dehydrogenase into an allosteric electrochemical Ca^{2+} sensor with simple amperometric glucometer readout.[22] The strategy of redox polymer enzyme immobilization, widely used to electrically couple redox proteins to sensitive electrochemical platforms[23,24], has also not been explored in combination with allosteric redox enzymes for advanced biosensor construction with signal amplification.

Based on the above, the first objective of this proof-of-principle study was to demonstrate that allosteric redox enzymes can be coupled to signal-generating electrode surfaces by embedding them within redox polymer films with properly adapted mass transport properties and formal potential, $E^{o,\prime}$. The redox enzyme chosen for this work was the allosteric flavin mononucleotide (FMN)-dependent reductase element (C1) of a two-component *p*-hydroxy-phenylacetate (*p*-HPA)-3-hydroxylase (HPAH) from the soil-based microorganism *Acinetobacter (A.) baumannii*. The second component (C2) of HPAH is a monooxygenase that hydroxylates the substrate *p*-HPA to 3,4 dihydroxy-phenylacetate (DHPA), the final product.[25,26] C1 and C2 are separate proteins which operate independently in terms of their biocatalytic functions. However, for conversion of *p*-HPA to DHPA their activities are coordinated through the activation of NADH oxidation by C1.[27–29]. In the context of this study it is important that although C1 does not use *p*-HPA as a substrate, *p*-HPA can bind to C1 and act as an effector to increase the rate of NADH oxidation (for a more detailed description of the mechanism see Supporting information, Eq. 1-3). Transient kinetic data show that allosteric modulation of C1 by *p*-HPA occurs by increasing the binding affinity for NADH and thus increasing the rate of NADH oxidation (≈20fold increase).[27] Therefore, the C1 reductase serves as a suitable allosteric model for inclusion into redox polymer biosensor preparations (refer to Eq. 4 in Section 1 of the Supporting Information).

Tangled polymer strings with electroactive side group attachments (so-called 'redox polymers') are widely used components of reagent-less biosensors [23,24]. An advantage in analyte signaling is that the physiochemical properties of the special polymers (such as their degree of hydrophobicity, general ionic charge identity and acidity, swelling capability etc.) and their $E^{o,\prime}$ standards can be matched to the target enzyme by use of an optimized macromolecule backbone and electroactive mediator design, respectively [24,30]. A useful type of covalently fused mediator species in redox polymers are osmium (III) complexes bearing imidazole or pyridine based ligands, since formal potentials are adjustable over a wide range through the introduction of electron-donating or electron-withdrawing groups in the ligand periphery of the metal cation.[24,30]. A Covalent anchoring of the mediator to a backbone polymer chain prevents mediator leaching, the escape of redox units into the measuring solution during sensor operation, which is an important issue with respect to signaling reliability and long term stability[31]. Examples of electrodes with Os-complex modified redox polymer/enzyme modifications range from amperometric biosensors for the quantification of glucose[32–36], lactate[34] and aldehydes[37] to simple enzymic detectors of hydrogen peroxide[34,38].

Here, our exemplary redox enzyme, the bacterial reductase C1 from *A. baumannii*, was incorporated in Os-complex modified redox polymer electrode coatings, with $E^{o,\prime}$ adaptations for effective faradaic communication between the FMN unit of the redox enzyme and the transition metal complexes tethered to macromolecular chains. C1/redox polymer-based biosensors were demonstrated to work well for the detection and quantification of NADH in amperometric mode, with sensor signals amplifiable through allosteric C1 stimulation by *p*-HPA.

EXPERIMENTAL SECTION

Materials and Methods

Chemicals, materials and solvents of reagent or higher grade were from Alfa-Aesar, Sigma-Aldrich, Acros-Organics, Deutero, Euriso-top SAS, Merck or VWR International. Solvents for NMR spectroscopy were stored at 4 °C. Deuterated DMSO-d_6 was stored at room temperature. Prior to use, chemically stabilized monomers for polymer synthesis were passed through short columns packed with the corresponding inhibitor remover and then stored at -20 °C or 4 °C. The monomer 4-vinylbenzenesulfonate was used as received. The polymer poly(4-vinylpyridine) (PVP, 160 kDa) was purchased from Sigma-Aldrich and used without any pretreatment. Polymeriza-

tion initiator 2,2′-azobis (2-methylpropio-nitrile) (AIBN) was recrystallized from hot toluene or methanol and then kept at -20 °C or 4 °C. All aqueous buffer and stock solutions were prepared with ultrapure deionized water. The Os-precursor K_2OsCl_6 was purchased from Sigma (grade: metal content of > 50 %). Dry organic solvents were purchased from Acros-Organics (AcroSeal bottles containing molecular sieves). The substrate β-nicotinamide adenine dinucleotide (NADH, reduced disodium salt hydrate) and the allosteric modulator para-hydroxyphenylacetate (*p*-HPA) were purchased from Acros Organics. The crosslinker poly (ethylene glycol) diglycidyl ether (PEGDGE, number average molecular weight, M_n, 400 Da) was purchased from Sigma-Aldrich, and used as an aqueous solution (11.40 mg mL^{-1}). Stock solutions of NADH (50 mM) and *p*-HPA (10 mM) were made with Tris-buffer (10 mM, pH 10) and PBS (50 mM, pH 7), respectively. The NADH solution was stored at 4 °C.

All reactions and manipulations were carried out using standard Schlenk techniques except where otherwise noted. NMR experiments were conducted with a DPX200 spectrometer from Bruker with a ^1H and ^{13}C resonance frequency of 200.13 MHz and 50.32 MHz, respectively. The residual solvent peak served as internal standard. All UV-vis absorption spectra were recorded with a Cary 60 photo-spectrometer from Agilent, using quartz or polystyrene cuvettes with an optical path length of 1 cm. All electron ionization (EI) mass spectrometric experiments were performed with a VG Autospec spectrometer (Jeol).

Electrochemical Experiments

All electrochemical experiments were conducted with a CHI 1030 multichannel potentiostat (CH Instruments) or a PalmSens3 potentiostat using a standard three-electrode setup under argon atmosphere and at room temperature in a conventional electrochemical glass cell (working volume ≈ 4 mL). A Pt-wire was used as the counter electrode and the Ag/AgCl/3 M KCl system served as the reference electrode. For measurements with the free Os-complex glassy carbon electrodes (3 mm, sealed in PEEK, BAS) were used as working electrodes. For all other measurements the working electrodes were 3 mm graphite rods (SGL Carbon), wrapped with PTFT tape to minimize background currents. For measurements with the free Os-complex an 1 M KCl/water solution was used as working electrolyte. For all other experiments PBS (50 mM, pH 7) was used as working electrolyte. Unless otherwise noted, dissolved oxygen was removed from electrolytes by 30 min of argon bubbling prior to measurements and deaeration was maintained during test trials by maintenance of an argon atmosphere above the electrolyte. For all chronoamperometric experiments a constant potential of -0.1 V vs. Ag/AgCl/3 M KCl was applied. Cyclic voltammograms were not corrected for background. Graphite and glassy carbon electrodes were thoroughly polished and rinsed with ethanol and water prior to measurements/modification.

All polymer and enzyme/polymer modified electrodes were prepared by a standard drop-cast process. The preparation of the PVP-Os/C1 modified electrodes was conducted as follows: 4 µL of C1 in 50 mM PBS, pH 7 (36.4 mg mL^{-1}), 4 µL of PEGDGE in water (11.40 mg mL^{-1}), 5 µL of PVP-Os in water (46.5 mg mL^{-1}) and 7.0 µL of PBS (50 mM, pH 7.0), giving a mass ratio of 3:1:5 of C1/PEGDGE/PVP-Os, were thoroughly mixed and 5 µL of this solution (with overall concentrations of 12 mg mL^{-1} polymer, 2.28 mg mL^{-1} crosslinker and 7.3 mg mL^{-1} enzyme) were drop-cast onto the graphite disk electrode and allowed to dry. For electrodes prepared without the crosslinker PEGDGE, 5.0 µL of PVP-Os (46.5 mg mL^{-1} in water), 4.0 µL of C1 (36.4 mg mL^{-1} in PBS) and 11 µL of PBS (50 mM, pH 7) were mixed and 5 µL of this solution (with 12 mg mL^{-1} polymer and 7.3 mg mL^{-1}) was drop-cast onto the graphite electrode. For the preparation of the P(SS-GMA-BA)-Os/C1 electrodes, 7.5 µL of P(SS-GMA-BA)-Os in water (16 mg mL^{-1}), 4.0 µL of C1 in PBS (36.4 mg mL^{-1}) and 8.5 µL of 50 mM PBS (pH 7.0) were mixed and 5 µL of this solution (with overall concentrations of 6 mg mL-1 polymer and 7.3 mg mL^{-1} enzyme) were drop coated onto a graphite electrode. The modified electrodes were dried for 2 h under ambient conditions and then stored at 4 °C until use.

Allosteric redox enzyme preparation

Previously described protocols were used to isolate and purify the allosteric p-hydroxy-phenylacetate reductase from *A. baumannii* (C1).[25,26]. The primed enzyme stock for this study contained 36.4 mg mL^{-1} protein in 50 mM PBS (pH 7) and was stored frozen at -20 °C.

Redox polymer synthesis

A detailed description of all syntheses as well as characterization of the compounds is provided in the Supporting Information. The synthesis of the hexanoic acid-modified poly(4-vinylpyridine) backbone (PVP-C6-acid) for the covalent binding of the Os-complex based mediator was described earlier,[39] as was the preparation of 2,2′-biimidazole (compound **3**, Scheme S1) and ligand *N*-(6-aminohexyl)-*N*′-methyl-2,2′-biimidazole (compound **4**, Scheme S1).[36,40] The preparation of the polymer backbone P(SS-GMA-BA) was adapted from protocols described in ref. [41].

RESULTS AND DISCUSSION

C1 reductase to electrode wiring through embedding in Os(III)-complex modified redox polymers

The reductase component C1 of the *p*-HPA-3-hydroxylase uses FMN as redox cofactor in the oxidation of NADH. Hence, for the electrical wiring of this enzyme two prerequisites have to be fulfilled by the redox matrix: first, the potential of the redox mediator has to be low enough to avoid significant oxidation of NADH at the mediator

and at the electrode (note that the electrode potential has to be adjusted to the potential of the mediator); and second, the potential has to be considerably more positive than that of the FMN coenzyme, to ensure fast electron transfer between the enzyme and the mediator.

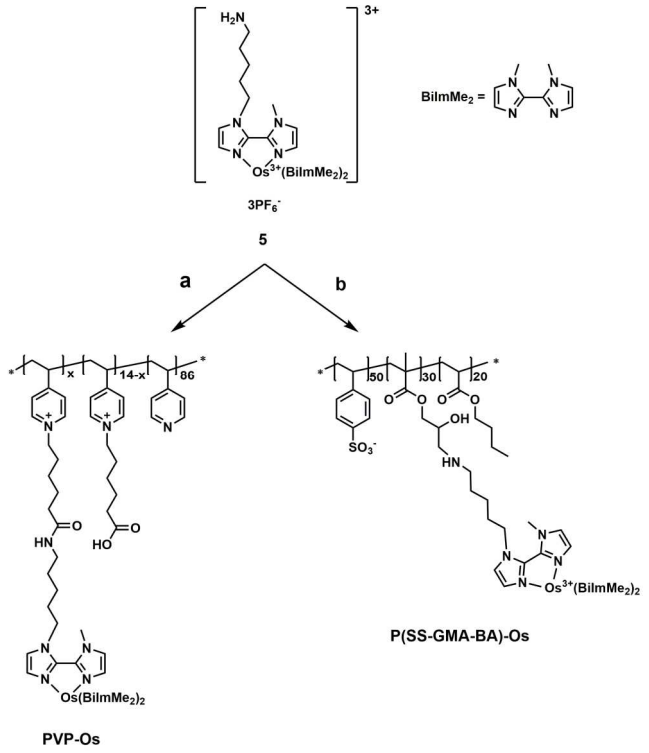

Scheme 1: Synthesis of the redox polymers PVP-Os and P(SS-GMA-BA)-Os. Complex **5** has a primary amino group within its ligand periphery, which can be used to covalently attach the complex to activated acid functions in PVP-C6-acid to yield PVP-Os.[36] At elevated temperatures and with a base catalyst the amino group can also react with electrophilic epoxide functions in P(SS-GMA-BA) to form P(SS-GMA-BA)-Os. Reaction conditions: (a) dry dimethylformamide, PVP-C6-acid, TSTU, DIPEA, room temperature, argon, overnight; (b) water/DMSO, P(SS-GMA-BA), NaOH as base catalyst., 50 °C, overnight.

Since significant oxidation of NADH at graphite electrodes occurs only at potentials > -100 mV vs. Ag/AgCl/3 M KCl (Figure S1) and the potential of the FMN domain is rather negative (≈ -400 mV vs. Ag/AgCl/3 M KCl, depending on the protein environment), the mediator should have a potential within these limits.

The potential of Os-complexes can easily be tuned by the coordination of either electron-withdrawing or electron-donating ligands to the metal center. [42] Mao et al. reported the synthesis of the low potential Os-complex (**5**, Scheme 1, top) bearing three biimidazole-based ligands, which results in a redox potential of around -240 mV vs. Ag/AgCl/3 M KCl (see ref. [36] and Figure S2A). This potential is within the above-mentioned limits. Consequently, this mediator should be suitable for chronoamperometric experiments, interacting with the C1 unit at applied potentials that do not cause simultaneous NADH oxidation at the electrode. For polymer preparation, this mediator was attached to two different backbones to yield the redox polymers PVP-Os and P(SS-GMA-BA)-Os (Scheme 1, bottom). The synthesis of PVP-Os, described by Mao et al. [36], was originally used for the electrical wiring of glucose oxidase. In PVP-Os, the mediator is attached to a hexanoic acid-modified poly(4-vinlypyridine) backbone (PVP-C6-acid) by activation of the acid moieties with *N*,*N*,*N*′,*N*′-tetramethyl-*O*-(*N*-succinimidyl) uronium tetrafluoroborate (TSTU) and the subsequent reaction of the active ester with complex **5** by amide formation (Scheme 1 and Scheme S2). The novel polymer P(SS-GMA-BA)-Os was synthesized starting from the co-polymer P(SS-GMA-BA), which contains electrophilic epoxide functions within the backbone (for synthesis see supporting information and Scheme S3). The epoxides can be used as anchoring sites for attachment of complex **5,** by inducing a ring-opening reaction of the -COC- moiety with the primary amino group in **5** at elevated temperature, using a base catalyst (Scheme 1 and Scheme S3). Polymer PVP-Os has a positively charged backbone due to the alkylated pyridine moieties. In contrast, P(SS-GAM-BA)-Os has a negatively charged backbone, due to the sulfonate groups in the styrene-based co-monomer (Scheme 1: note that at pH 7 the sulfonate groups are fully ionized). Both polymers are very hydrophilic and thus provide a solvated environment for the reductase C1. The redox potentials of the modified polymers were estimated from cyclic voltammograms, measured with drop-cast films in phosphate buffered saline (PBS, 50 mM) at pH 7, to be -190 mV (PVP-Os) and -220 mV (P(SS-GMA-BA)-Os) vs. Ag/AgCl/3 M KCl (Figures S2B and C). From a thermodynamic point of view, both polymers should be able to extract electrons from the FMN dependent C1 and are below the oxidation potential of NADH at graphite electrodes. Indeed, cyclic voltammograms (Figure 2) of graphite electrodes modified with PVP-Os/C1 (A) and P(SS-GMA-BA)-Os/C1 (B) films showed a well-defined catalytic response upon the addition of the substrate NADH, according to the mechanism depicted in Figure 1. To avoid artefacts caused by interfering O_2 all experiments with polymer/enzyme films were conducted in argon saturated electrolytes under argon atmosphere, since the low potential Os-complex catalyzes the oxygen the oxygen reduction reaction[35] and O2 represents the natural electron acceptor for the isolated C1 unit[43].

Compared to the anionic polymer backbone in P(SS-GMA-BA)-Os, the positively charged polymer PVP-Os supported much higher catalytic currents at, for instance, a NADH concentration of 5 mM (cf. Figures 2A and B, red traces). The charge at the polymer base chain apparently influenced the strength of the C1/Os-complex interaction within the matrix and the efficiency of the process was

higher in the presence of alkylated cationic pyridine moieties, even with an identical positively charged Os-complex based mediator, probably because of the net surface charge of the enzyme molecules, which at pH = 7 is predominantly negative (pI 6.02, calculated with the ExPASy - SIB Bioinformatics Resource Portal, GenBank ID: OUM80372.1).

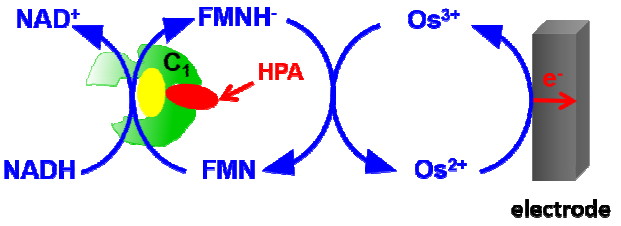

Figure 1: Simplified schematic of the electrical wiring of reductase C1 under substrate turnover conditions (in presence of NADH) via an Os(III)-complex modified redox polymer. For clarity, only the Os-metal centers and their corresponding oxidation states are shown. The allosteric effector *p*-HPA can bind to regulatory sites on C1, inducing a conformational change in the enzyme that affects the substrate-binding site. This increases the rate of conversion of NADH to NAD^+, which is observable as an increase in Os (II) oxidation current.

Repulsive forces between entrapped enzyme and the negatively charged backbone in P(SS-GMA-BA)-Os thus may hinder the optimal spatial arrangement of the redox site of the polymer and the biocatalyst, compared to the cationic PVP-Os sensor. This emphasized the importance of the rational design of the redox polymer in achieving effective electrical wiring of the C1 biocatalyst and confirmed similar fundamental findings for other proteins.[24,30,44] Nevertheless, both polymers tested were able to exchange electrons with C1, though with significantly different efficiencies, which proved that the bacterial reductase could be functionally connected to an electrode surface by means of a redox polymer. Repetitive cyclic voltammograms, acquired with both polymer/enzyme electrodes, showed a stable current response over several cycles (Figure S3).

It is known that Os-complex modified polymers can mediate the oxidation of hydroquinones.[45,46] Hence, the contribution of Os-complex mediated oxidation of NADH (electronic structure is similar to those of quinones) was evaluated, to ensure that the detected current response was solely or mainly based on electrical communication between the polymer and the biocatalyst. In these tests pure redox polymer was drop-coated onto graphite electrodes and cyclic voltammograms were recorded in the absence and presence of NADH. PVP-Os-modified sensors produced a weak anodic current upon addition of NADH (Figure S4A) while P(SS-GMA-BA)-Os was virtually unresponsive to this (Figure S4B). For both polymer coatings, however, a slight current elevation at potentials above -50 mV vs. Ag/AgCl/3 M KCl was observed, indicating some oxidation of NADH directly at the graphite electrode surface.

Finally, we evaluated the contribution to the response by direct electron transfer (DET) from the enzyme to the electrode, with C1 immobilized by absorption on the electrode surface by a drop-coating process.

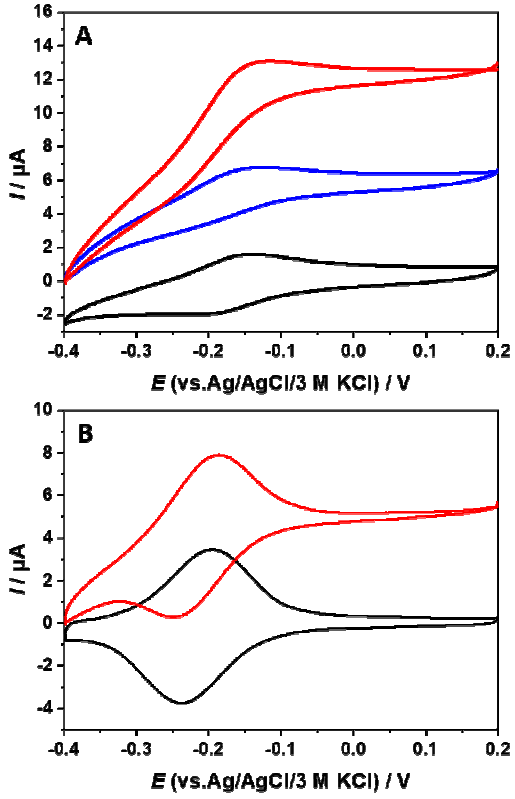

Figure 2: Cyclic voltammograms of PVP-Os/C1 (A) and P(SS-GMA-BA)-Os/C1 (B) graphite electrode modifications in the absence (black traces) and presence of NADH (2.5 mM: blue trace, 5 mM: red traces); working electrolyte: deaerated PBS (50 mM, pH 7); all *I*/*E* curves were recorded at a scan rate of 2 mV s^{-1}.

Cyclic voltammograms showed only a weak anodic current at potentials above -300 mV vs. Ag/AgCl/3 M KCl (Figure S5, blue trace), indicating that very little electron transfer occurred between the redox-active protein and the graphite electrode. Not surprisingly, adsorption of C1 alone formed poorly stable enzyme films on the electrode surface. The use of a stabilizing immobilization matrix, i.e. the hydrophilic P(SS-GMA-BA) polymer backbone without bound Os-complexes, increased the signal stability but did not lead to higher catalytic currents (red trace in Figure S5).

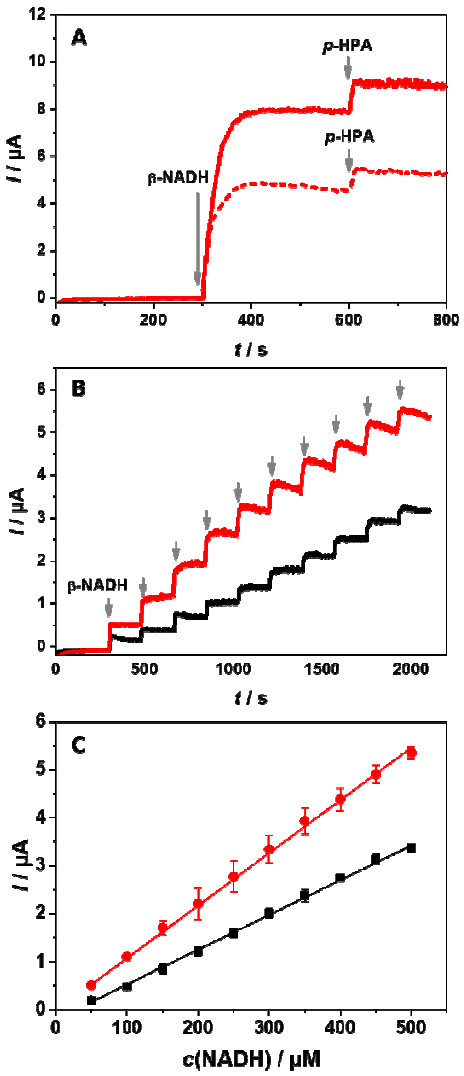

Figure 3: Effect of the allosteric effector *p*-HPA on the amperometric detection of NADH with PVP-Os/C1 modified electrodes. A: Chronoamperograms for different NADH concentrations (dashed line: 0.5 mM, solid line: 1 mM, added at t = 300 s) in the presence of *p*-HPA (500 µM, added at t = 600 s). B: Chronoamperograms at PVP-Os/C1 electrodes for NADH concentrations in the range of 50 – 500 µM in the absence (black curve) and presence of 100 µM *p*-HPA (red curve); with each addition of NADH stock solution (grey arrows) the concentration of the substrate was increased by 50 µM. C: I/c calibration plots for NADH detection in the presence (red filled circles) and absence (black filled circles) of *p*-HPA (100 µM). Red data points correspond to current values measured prior to each subsequent NADH addition. The difference in the slopes of the red (11 nA μM^{-1}) and black (7 nA μM^{-1}) linear regression lines shows the increase in biosensor sensitivity through allosteric C1 activation. Error bars are standard deviations for triplicate repetitions of measurements in PBS, 50 mM, pH 7 at a working electrode potential of -100 mV vs. Ag/AgCl/3 M KCl.

To demonstrate that indeed a mediated electron transfer mechanism is present and to evaluate the contribution of DET to the detected catalytic currents, a polymer double layer, composed of an underlying C1-free PVP-Os layer and an active PVP-Os/C1 upper layer, was introduced to prevent contact of the protein with the electrode surface.

For valid comparison with single layer sensor responses, the absolute amount of immobilized PVP-Os in double layer sensor variants was adjusted to equal that in PVP-Os/C1-modified graphite electrodes. Cyclic voltammetry was again used to analyze the behavior of these polymer double layer electrodes. In the presence of NADH a clear catalytic wave was observed for the double-layer system (Figure S6A, red line), however, the catalytic current trace in the region of reaction onset was less steep than in the single layer system (blue line). The experiment provided further evidence of effective mediated electron transfer between C1 and the redox matrix since in the double layer configuration the C1 unit is not in direct contact with the electrode surface (DET is prevented).
At potentials above 0 V vs. Ag/AgCl/3 M KCl steady state catalytic currents were reproducibly slightly smaller for the double layer sensor system. The difference between the current traces for PVP-Os//PVP-Os/C1 and PVP-Os/C1-mofications visualizes the contribution of DET to C1 biosensor signaling at these high potentials and/or indicates a limitation by the electron transport within the enzyme-free underlying polymer layer. The latter effect seems to be more likely since chronoamperometric experiments with the double layer configuration show not only a decreased steady state current but also a slower rise of the current response that indicates diffusional limitation (Figure S6B). Moreover, at an applied potential of -100 mV vs. Ag/AgCl/3 M KCl contribution of DET is less significant (see Figure S5, cf. black and blue traces at -100 mV). Hence, we conclude that the lower steady state currents are rather limited by a slow electron transport within the underlying polymer layer than by DET effects.

The more mechanistic look at the elementary reaction steps of immobilized C1/redox polymer blends was followed by a detailed evaluation of the analytical performance of such biosensors for the amperometric detection of NADH, obviously with and without allosteric C1 activation. Because of a more favorable signal with regard to current magnitude and response time the chosen sensor layout for all further work was the single-layered PVP-Os/C1 configuration that has allosteric C1 enzyme entities fixed into an Os-complex loaded and positively charged redox polymer network.

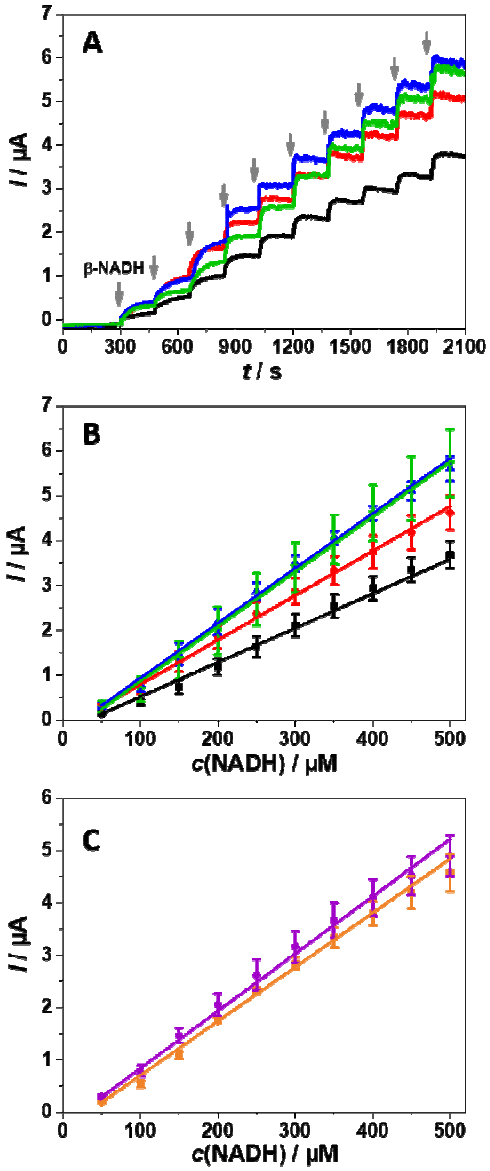

Figure 4: Performance characteristics of amperometric PEGDGE/PVP-Os/C1-based NADH biosensors. A: Chronoamperograms for analyte concentrations between 50 to 500 µM (grey arrows indicate incremental NADH additions of 50 µM) in the presence (red trace: 50 µM, blue trace: 100 µM, green trace: 150 µM) and absence (black line) of *p*-HPA. B: Calibration plots computed from the recordings in A; data points are the average values of four independent measurements (for color code see A). C: Calibration graphs obtained for pre-incubated PEGDGE/PVP-Os/C1-based NADH sensors; violet trace: 30 min incubation; orange trace: 10 min incubation; current values were extracted from traces shown in Figure S9. Values are the means of three independent measurements. For B and C, the error bars represent the calculated standard deviation of the fourfold (B) and triplicate (C) trials in 50 mM PBS, pH 7 at a working electrode potential of -100 mV vs. Ag/AgCl/3 M KCl.

In initial chronoamperometric measurements (Figure 3A) PVP-Os/C1-modified graphite electrodes responded reproducibly at a potential of -100 mV vs. Ag/AgCl/3M KCl to the addition of NADH with stepped increases in current, followed by subsequent progression to a new steady state (black trace: 0.5 mM and red trace: 1 mM). Supplementation of the electrolyte with the C1 effector *p*-HPA should induce another current step, through allosteric stimulation of the catalytic activity of C1. This is shown by the two *I-t* traces in Figure 3A, in which the addition of *p*-HPA to the buffer with pre-adjusted C1/NADH level produced the expected signal increase.

Calibration in amperometric mode were then carried out with the allosteric C1 biosensor assay for NADH concentrations between 50 and 500 µM in the 100 µM presence (Figure 3B, red trace) and absence (Figure 3B, black trace) of the allosteric activator *p*-HPA (note that within this concentration range the sensor shows a linear response for NADH oxidation; for higher concentrations, the current response deviates from a linear behavior, Figure S7). The current steps produced by incremental elevations of substrate concentration were consistently larger in the presence of *p*-HPA for all ten 50 µM additions (grey arrows), *p*-HPA producing a 1.5-fold increase in the sensitivity of amperometric NADH sensing, confirmed by the slopes of the corresponding calibration plots (Figure 3C, red and black traces). It was observed that the initial maximum current slowly declined with time (Figure 3B, red trace, valid from the 4th addition of substrate (200 µM) and Figure S8 even with a NADH concentration of 50 µM), most likely due to enzyme leaching and/or desorption of the polymer/enzyme film. To enhance the response stability of PVP-Os/C1-based NADH biosensors, bi-functional poly(ethylene glycol) diglycidyl ester (PEGDGE) was added as cross-linking agent to the immobilization layer. PEGDGE contains two electrophilic epoxide functions that readily react at room temperature with amino groups on protein surfaces.[47] Covalent attachment of C1 to PEGDGE within the immobilization layer was expected to achieve more stable fixation of the enzyme to the graphite electrodes. Moreover, entanglements between the PVP-backbone chains and the linear PEGDE crosslinker chains may also enhance the film stability (note that formation of *covalent* pyridine-epoxide adducts requires elevated temperatures[48,49] which were not applied for electrode preparation). NADH-selective C1 biosensors were prepared with different PEGDGE:PVP-Os:C1 ratios and optimal amperometric detection performance was obtained with 5 µL of PBS containing 2.3 mg mL^{-1} PEGDGE, 12.0 mg mL^{-1} PVP-Os and 7.3 mg mL^{-1} C1, dropped and dried on well-polished graphite precursor electrode disks. Representative amperometric recordings in the presence (Figure 4A, red, blue and green traces) and absence (black trace) of *p*-HPA revealed stable sensor responses to NADH, even at high concentrations. We want to emphasize that for the crosslinked films stable

steady state currents were observed for each NADH addition (Figure 4A) which was not the case for the non-crosslinked films (Figure 3B). Moreover, as was seen in the calibration plots of simple PVP-Os/C1 sensors, *p*-HPA also increased the sensitivity of the PEGDGE/PVP-Os/C1 biosensor (Figure 4B). Apparently, covalent crosslinking of C1 to PEGDGE chains improved the stability of C1 fixation without adversely affecting the mobility of the substrate, NADH, or the effector, *p*-HPA, within the immobilization layer. Comparison of the calibration plots for the three *p*-HPA concentrations (Figure 4C, red trace 50 µM, blue trace 100 µM and green trace 150 µM) showed a moderate concentration dependence for allosteric C1 activation, with the maximum stimulation reached at an effector concentration of 100 µM, equivalent to a 400-fold molecular excess of *p*-HPA molecules in the electrolyte solution over C1 units on the electrode.

The effect of the allosteric effector on the enzymes activity in the polymer film is less pronounced than in solution containing the freely diffusing species (≈20fold increase of the reaction rate[27]). This is most likely due to a limited diffusion and hampered binding of the allosteric effector and/or substrate in the hydrogel film or due to steric constraints in the polymer film. Nevertheless, as shown in Figure 3, a clear enhancement is still visible. Nevertheless, as shown in Figure 3, a clear enhancement is still visible.

For practical analytical applications, reagent-less biosensors are preferred. We therefore tried replacement of *p*-HPA in the electrolyte by a pre-incubation procedure that exposed the immobilized C1 to the stimulant ex situ before NADH analysis: PEGDGE/PVP-Os/C1-modified electrodes were immersed in PBS (50 mM, pH 7) containing 100 µM *p*-HPA, at room temperature for 10 or 30 min. Original current recordings of amperometric NADH measurements with PEGDGE/PVP-Os/C1 biosensors of the two conditions are shown in Figure S9, and the corresponding calibrations plots are depicted in Figure 4C. The anodic current steps on incremental additions of NADH are approximately independent of pre-incubation time (cf. violet and orange trace in Figure S9) but are significantly greater than those from biosensors untreated with *p*-HPA (see Figure 4A, black trace as example). Obviously, capture of allosteric effector molecules by binding sites in C1 occurred during the few min of pre-incubation and, as indicated by a lack of decay in the sensor response, the C1/*p*-HPA adducts were active throughout the 35-min chronoamperometric measurement.

Table 1 summarizes the sensitivities of the PEGDGE/PVP-Os/C1-based *NADH* biosensor in the various analytical protocols used in this study. The value was 12.1 nA μM^{-1} when the electrodes were continuously exposed to 100 µM allosteric effector. Pre-incubation in a PBS buffer with that concentration of *p*-HPA, however, was about 15% less efficient in increasing the sensitivity; however, since the response was stable on the time scale of the performance tests it seems that a reagent-less NADH biosensor incubation assay with allosteric signal amplification is indeed possible.

Table 1: Sensitivity of PEGDGE/PVP-Os/C1-based NADH biosensors: Effect of *in situ* exposure or pre-incubation with the C1 effector *p*-HPA. Values are the means of at least three independent measurements in 50 mM PBS, pH 7 at a working electrode potential of -100 mV vs. Ag/AgCl/3 M KCl and for NADH concentrations in the range 50 - 500 µM.

Type of *p*-HPA exposure	Sensitivity / nA μM^{-1}
No *p*-HPA	8.25 ± 0.89
50 µM *p*-HPA in solution	9.70 ± 1.10
100 µM *p*-HPA in solution	12.08 ± 0.64
150 µM *p*-HPA in solution	12.58 ± 1.19
incubation for 10 min in 100 µM *p*-HPA	10.13 ± 1.08
incubation for 30 min in 100 µM *p*-HPA	10.45 ± 0.97

The suitability of the developed PEGDGE/PVP-Os/C1 biosensing assay with allosteric enzyme activation for quantitative NADH analysis was finally evaluated by assays of model samples with a nominal analyte concentration of 50 µM. The recovery rate was determined by five-fold repetition of standard measurements in PBS (50 mM, pH 7) with addition of 100 µM *p*-HPA for allosteric activation of C1. Figure 5A, a representative example, is one of five original amperometric recordings, showing four stepped current increases on addition of NADH to the measurement buffer.

Figure 5B is a standard addition plot constructed from the data in Figure 5A. In this particular case, the NADH sample concentration determined was 51.7 µM, equivalent to a recovery rate of 103.4 %, for the 50 µM sample. The average recovery rate for the five NADH quantifications was, 105.1 ± 4.5 % (52.5 ± 2.1 µM: see Table S1 for the individual values), which demonstrated that allosterically activated C1 in a PEGDGE/PVP-Os mixture worked efficiently and reproducibly for accurate quantitation of NADH.

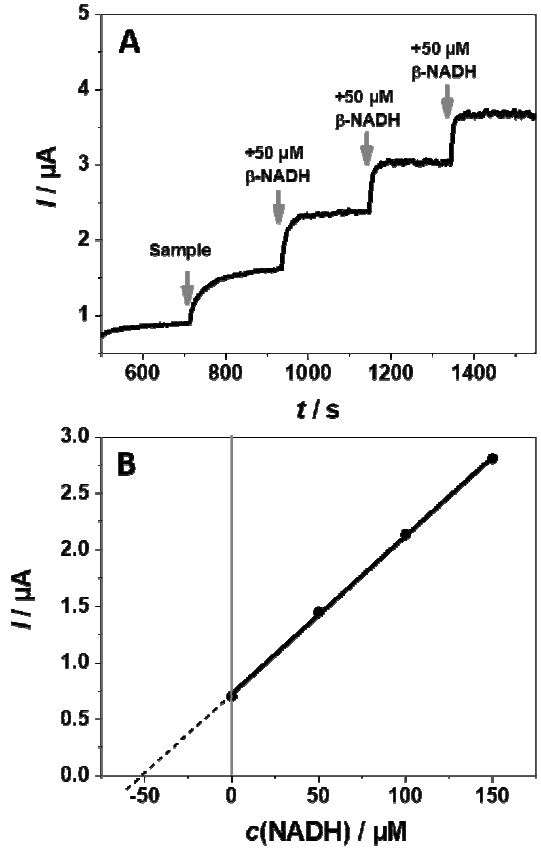

Figure 5: Detection of NADH with a PVP-Os/C1/PEGDGE electrode used in the standard addition mode. A: Representative chronoamperogram for with an initial addition of 50 µM NADH ("sample") and three subsequent 50 µM additions. The electrolyte was 50 mM PBS, pH 7 and the working electrode potential was -100 mV vs. Ag/AgCl/ 3 M KCl. B: Standard addition plot constructed with the data of the I/t curve in A) and evaluation of the test concentration (51.7 µM), and the recovery (103.3 %) from the linear regression line.

From the standard deviation of the background current (8 blank measurements) in chronoamperometric experiments and with the linear regression of the *I-c* curves (sensitivity, see Table 1) the limit of detection (LOD) in the presence (100 µM) and absence the allosteric effector p-HPA was estimated to be 14 µM and 15 µM, respectively. Both values are only about one order of magnitude higher than values obtained with rather classical amperometric NADH-detectors based on redox active (0.2 – 1.0 µM)[50] or conducting polymers (0.76 µM)[51], polymer modified nanoparticles (0.1 µM)[52], graphene (1.4 -1.5 µM)[53,54] or polymer/enzyme films (0.08 µM)[55]. However, this was the first approach that describes NADH detection via the allosteric activation of a polymer embedded redox enzyme.

Measurements drastically exceeding the timescale of the standard voltammetric and chronoamperometric experiments show a significant current decrease over time. Moreover, reused electrodes showed a lower current response than freshly prepared sensors. Thus, we conclude that the developed sensor is suitable for single-use only. Nevertheless, the electrodes show good recovery rates and demonstrated high reproducibility.

Apparently, the redox wiring of C1 to and its stable and biocompatible entrapment on the transducer electrode were both accomplished through the strategy of using a specially tailored redox polymer/crosslinker composite as immobilization matrix.

CONCLUSION

We have described the previously unreported functional addition of an allosteric enzyme, namely the NADH-specific C1 reductase subunit of a bacterial *p*-hydroxylphenylacetate hydroxylase, to a redox polymer thin film on voltammetric electrodes. The choice of a suitable PVP-Os-based redox polymer with matching formal potential, with the additional integration of the polymeric crosslinker PEGDGE, produced amperometric C1 biosensors that, in deaerated measuring buffers to prevent oxygen acting as an electron-acceptor partner for redox regeneration, detected the C1 substrate, NADH, at a working potential adjusted for Os(II) to Os(III) oxidation. The observation of NADH-dependent signals was evidence for efficient electrical redox wiring from C1 along a trail of complexed metal ions in the polymer film to the transducer surface, here a graphite disk. Furthermore, supplementation of the measuring buffer with *p*-HPA, an allosteric activator of C1, increased the rate of substrate conversion by the immobilized biocatalyst and amplified the current response to a given NADH concentration. The C1/*p*-HPA couple showed an approximately 1.5-fold increase of sensitivity in amperometric NADH analysis, compared to sensor operation in absence of the allosteric activator, and activation by pre-incubation suggested the feasibility of a reagent-less version of the allosterically enhanced NADH biosensor.

This proof-of-principle study showed, for the first time, the feasibility of allosteric activation of a sensor surface-attached enzyme within an immobilizing redox polymer layer. The proposed approach should also be applicable to other redox enzymes, and the exploitation of molecular regulation of sensor performance and the modulation of enzyme anodes and cathodes of biofuel cells can be anticipated.

ASSOCIATED CONTENT

Supporting Information

Additional electrochemical experiments and controls. Electrochemical and spectroscopic characterization of the redox polymers and precursors. Additional sensor characteristics. Detailed protocols for syntheses of the redox polymers and precursors.

AUTHOR INFORMATION

Corresponding Authors

*Phone: +49-234-3225586 (A.R.); +66-8737-58518 (A.S.).
*Email: adrian.ruff@ruhr-uni-bochum.de (A.R.); albert.s@vistec.ac.th (A.S.).

Author Contributions

The manuscript was written through contributions of all authors. All authors have given approval to the final version of the manuscript.

Notes

The authors declare no competing financial interest.

ACKNOWLEDGMENTS

The authors are grateful for the core financial support of this work by the Thailand Research Fund through a grant from the respected Royal Golden Jubilee Ph.D. Program with Grant No. PHD/0160/2557 and for supportive "Biochemistry-Electrochemistry Research Unit" budget allocations of Suranaree University of Technology to A.S. and W.S, in particular in the frame of the Center of Excellence (CoE) in Advanced Functional Materials, Institute of Science, Suranaree University of Technology, Nakhon Ratchasima 30000, Thailand. A.R., S. J. and W.S. are grateful to the Deutsche Forschungsgemeinschaft (DFG) for funding within the framework of the Cluster of Excellence RESOLV (EXC1069) and the European Commission within the Marie-Curie project "Bioenergy" (PITN-GA-2013-607793). Research in the P.C. lab was supported by a grant from The Thailand Research Fund (RTA5980001). The authors thank Sarra Zerria for her help with redox polymer syntheses and Dr. David Apps, quondam Reader, Centre for Integrative Physiology, Edinburgh Medical School: Biomedical Sciences, Edinburgh, Scotland, for his critical manuscript reading and language improvements.

REFERENCES

(1) Swain, J. F.; Gierasch, L. M. *Curr. Opin. Struct. Biol.* **2006**, *16*, 102–108.
(2) Villaverde, A. *FEBS Lett.* **2003**, *554*, 169–172.
(3) Zhu, L.; Anslyn, E. V. *Angew. Chem. Int. Ed.* **2006**, *45*, 1190–1196.
(4) Marvin, J. S.; Corcoran, E. E.; Hattangadi, N. A.; Zhang, J. V.; Gere, S. A.; Hellinga, H. W. *Proc. Nat. Acad. Sci. U.S.A.* **1997**, *94*, 4366–4371.
(5) Soukup, G. *Trends Biotechnol.* **1999**, *17*, 469–476.
(6) Zorn, J. A.; Wells, J. A. *Nat. Chem. Biol.* **2010**, *6*, 179–188.
(7) Di Cera, E. *Method. Enzymol.*, *466*, 259–271.
(8) Li, J.; Gierach, I.; Gillies, A. R.; Warden, C. D.; Wood, D. W. *Biosens. Bioelectron.* **2011**, *29*, 132–139.
(9) Meister, G. E.; Joshi, N. S. *ChemBioChem* **2013**, *14*, 1460–1467.
(10) Ferraz, R. M.; Rodríguez-Carmona, E.; Ferrer-Miralles, N.; Meyerhans, A.; Villaverde, A. *J. Mol. Recognit.* **2009**, *22*, 255–260.
(11) Ferraz, R. M.; Arís, A.; Villaverde, A. *Biotechnol. Bioeng.* **2006**, *94*, 193–199.
(12) Ricci, F.; Vallée-Bélisle, A.; Porchetta, A.; Plaxco, K. W. *J. Am. Chem. Soc.* **2012**, *134*, 15177–15180.
(13) Han, L.; Liu, A. *ACS Appl. Maters Interfaces* **2017**, *9*, 6894–6901.
(14) Salehi, A. S. M.; Shakalli Tang, M. J.; Smith, M. T.; Hunt, J. M.; Law, R. A.; Wood, D. W.; Bundy, B. C. *Anal. Chem.* **2017**, *89*, 3395–3401.
(15) Reuel, N. F.; McAuliffe, J. C.; Becht, G. A.; Mehdizadeh, M.; Munos, J. W.; Wang, R.; Delaney, W. J. *ACS Sens.* **2016**, *1*, 348–353.
(16) Lifschitz, A. M.; Rosen, M. S.; McGuirk, C. M.; Mirkin, C. A. *J. Am. Chem. Soc.* **2015**, *137*, 7252–7261.
(17) Vlatković, M.; Collins, B. S. L.; Feringa, B. L. *Chem. Eur. J.* **2016**, *22*, 17080–17111.
(18) Wollenberger, U.; Scheller, F. W. *Biosens. Bioelectron.* **1993**, *8*, 291–297.
(19) Mast, N.; Anderson, K. W.; Johnson, K. M.; Phan, T. T. N.; Guengerich, F. P.; Pikuleva, I. A. *J. Biol. Chem.* **2017**, *292*, 12934–12946.
(20) Haber, A.; Abu-Younis Ali, A.; Aviram, M.; Gross, Z. *Chem. Commun.* **2013**, *49*, 10917–10919.
(21) Wijma, H. J.; Macpherson, I.; Alexandre, M.; Diederix, R. E. M.; Canters, G. W.; Murphy, M. E. P.; Verbeet, M. P. *J. Mol. Biol.* **2006**, *358*, 1081–1093.
(22) Guo, Z.; Johnston, W. A.; Stein, V.; Kalimuthu, P.; Perez-Alcala, S.; Bernhardt, P. V.; Alexandrov, K. *Chem. Commun.* **2016**, *52*, 485–488.
(23) Heller, A. *Acc. Chem. Res.* **2002**, *23*, 128–134.
(24) Ruff, A. *Curr. Opin. Electrochem.* **2017,** DOI: 10.1016/j.coelec.2017.06.007.
(25) Chaiyen, P.; Suadee, C.; Wilairat, P. *Eur. J. Biochem.* **2001**, *268*, 5550–5561.
(26) Thotsaporn, K.; Sucharitakul, J.; Wongratana, J.; Suadee, C.; Chaiyen, P. *Biochim. Biophys. Acta* **2004**, *1680*, 60–66.
(27) Sucharitakul, J.; Chaiyen, P.; Entsch, B.; Ballou, D. P. *Biochemistry* **2005**, *44*, 10434–10442.
(28) Sucharitakul, J.; Phongsak, T.; Entsch, B.; Svasti, J.; Chaiyen, P.; Ballou, D. P. *Biochemistry* **2007**, *46*, 8611–8623.
(29) Phongsak, T.; Sucharitakul, J.; Thotsaporn, K.; Oonanant, W.; Yuvaniyama, J.; Svasti, J.; Ballou, D. P.; Chaiyen, P. *J. Biol. Chem.* **2012**, *287*, 26213–26222.
(30) Heller, A. *Curr. Opin. Chem. Biol.* **2006**, *10*, 664–672.
(31) Heller, A.; Feldman, B. *Chem. Rev.* **2008**, *108*, 2482–2505.
(32) Pinyou, P.; Ruff, A.; Pöller, S.; Ma, S.; Ludwig, R.; Schuhmann, W. *Eur. J. Chem.* **2016**, *22*, 5319–5326.
(33) Taylor, C.; Kenausis, G.; Katakis, I.; Heller, A. *J. Electroanal. Chem.* **1995**, *396*, 511–515.
(34) Lumley-Woodyear, T. de; Rocca, P.; Lindsay, J.; Dror, Y.; Freeman, A.; Heller, A. *Anal. Chem.* **1995**, *67*, 1332–1338.
(35) Prévoteau, A.; Mano, N. *Electrochim. Acta* **2012**, *68*, 128–133.
(36) Mao, F.; Mano, N.; Heller, A. *J. Am. Chem. Soc.* **2003**, *125*, 4951–4957.
(37) Badalyan, A.; Dierich, M.; Stiba, K.; Schwuchow, V.; Leimkühler, S.; Wollenberger, U. *Biosensors* **2014**, *4*, 403–421.
(38) Suraniti, E.; Ben-Amor, S.; Landry, P.; Rigoulet, M.; Fontaine, E.; Bottari, S.; Devin, A.; Sojic, N.; Mano, N.; Arbault, S. *Angew. Chem. Int. Ed.* **2014**, *53*, 6655–6658.
(39) Ruff, A.; Pinyou, P.; Nolten, M.; Conzuelo, F.; Schuhmann, W. *ChemElectroChem* **2017**, *4*, 890–897.

(40) Alsaoub, S.; Ruff, A.; Conzuelo, F.; Ventosa, E.; Ludwig, R.; Shleev, S.; Schuhmann, W. *ChemPlusChem* **2017**, *82*, 576–583.
(41) Lopez, F.; Ma, S.; Ludwig, R.; Schuhmann, W.; Ruff, A. *Electroanalysis* **2017**, *29*, 154–161.
(42) Guschin, D. A.; Castillo, J.; Dimcheva, N.; Schuhmann, W. *Anal. Bioanal. Chem.* **2010**, *398*, 1661–1673.
(43) Sucharitakul, J.; Tinikul, R.; Chaiyen, P. *Arch. Biochem. Biophys.* **2014**, *555-556*, 33–46.
(44) Milton, R. D.; Hickey, D. P.; Abdellaoui, S.; Lim, K.; Wu, F.; Tan, B.; Minteer, S. D. *Chem. Sci.* **2015**, *6*, 4867–4875.
(45) Gregg, B. A.; Heller, A. *J. Phys. Chem.* **1991**, *95*, 5970–5975.
(46) Vering, T.; Schuhmann, W.; Seiwald, D.; Schmidt, H.-L.; Speiser, B.; Ye, L. *J. Electroanal. Chem.* **1994**, *364*, 277–279.
(47) Vasylieva, N.; Barnych, B.; Meiller, A.; Maucler, C.; Pollegioni, L.; Lin, J.-S.; Barbier, D.; Marinesco, S. *Biosens. Bioelectron.* **2011**, *26*, 3993–4000.
(48) Dell'Erba, I. E.; Williams, R. *Polym. Eng. Sci.* **2006**, *46*, 351–359.
(49) Xue, G.; Ishida, H.; Koenig, J. *Polymer* **1986**, *27*, 1134–1137.
(50) Gründig, B.; Wittstock, G.; Rüdel, U.; Strehlitz, B. *J. Electroanal. Chem.* **1995**, *395*, 143–157.
(51) Jaraba, P.; Agüí, L.; Yáñez-Sedeño, P.; Pingarrón, J. *Electrochim. Acta* **1998**, *43*, 3555–3565.
(52) Keeley, G. P.; O'Neill, A.; Holzinger, M.; Cosnier, S.; Coleman, J. N.; Duesberg, G. S. *PhysChemChemPhys* **2011**, *13*, 7747–7750.
(53) Li, L.; Lu, H.; Deng, L. *Talanta* **2013**, *113*, 1–6.
(54) Manesh, K. M.; Santhosh, P.; Gopalan, A.; Lee, K. P. *Talanta* **2008**, *75*, 1307–1314.
(55) Tang, X.; Johansson, G. *Anal. Lett.* **1995**, *28*, 2595–2606.

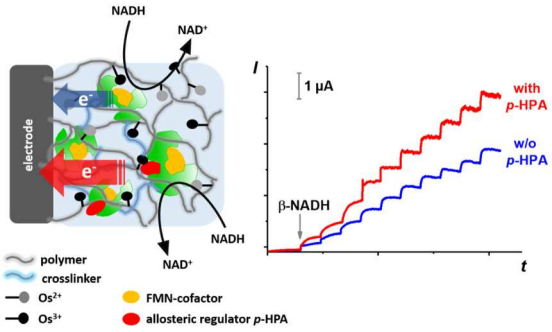

for TOC only